NEUROIMAGE **8,** 307–326 (1998)
ARTICLE NO. NI980365

Biophysical Linkage between MRI and EEG Coherence in Closed Head Injury

R. W. Thatcher,*,†,‡ C. Biver,‡ R. McAlaster,‡ and A. Salazar‡

*VA Medical Center, Research and Development Service, Bay Pines, Florida 33744; †Departments of Neurology and Radiology, University of South Florida College of Medicine, Tampa, Florida 33612; and ‡Defense and Veterans Head Injury Program, Washington, D.C.

Received March 11, 1998

Using conventional MRI procedures, nuclear magnetic resonance (NMR) of brain water proton (^{1}H) $T2$ relaxation times and EEG coherence were obtained from two independent groups of closed head injured (CHI) patients and a group of normal control subjects. Statistically significant intercorrelations were observed between ^{1}H $T2$ relaxation times of the cortical gray and white matter and EEG coherence. The analyses showed that lengthened ^{1}H $T2$ relaxation times of the cortical gray and white matter were related to: (1) decreased EEG coherence between short interelectrode distances (e.g., 7 cm) and increased EEG coherence between long interelectrode distances (e.g., 28 cm), (2) differences in EEG frequency in which $T2$ relaxation time was most strongly related to the gray matter in the delta and theta frequencies in CHI patients, and (3) increased $T2$ relaxation time and decreased short-distance EEG coherence were related to reduced cognitive function. The results were interpreted in terms of reduced integrity of protein/lipid neural membranes and the efficiency and effectiveness of short- and long-distance neural synchronization following traumatic brain injury.

Key Words: **EEG coherence; MRI; ^{1}H proton relaxation times; cognition; traumatic brain injury.**

1. INTRODUCTION

A biophysical linkage to the microenvironments of the neural cytoplasm, the myelin, and the extracellular space is important in the integration of the MRI to the electroencephalogram (EEG) and possibly other imaging modalities (Thatcher, 1995; Thatcher *et al.,* 1998). In the present paper a conventional spin-echo technique of MR imaging is used to derive the biophysical relaxation times ($T2$) of water protons located within the cortical gray matter and white matter. According to NMR studies (Schoeniger *et al.,* 1994; Doe and Snyder, 1995; Szafer *et al.,* 1995) the $T2$ relaxation times of water protons are dependent on the total concentration of water protons [^1H] or proton density located within different tissue compartments where [^1H] = [I] + [M] + [E]. [I] is defined as the concentration of intracellular water protons within the cortical cytoplasm (i.e., within the cytoplasm of the glia, axons and neural dendrites and cell bodies), [M] is defined as the concentration of water protons within the cortical myelin and, [E] is defined as the concentration of water protons that are in the extracellular space, e.g., cerebral spinal fluid (CSF) and the very small spaces between axons, neurons, and between glia and neurons (Nicholson, 1980; Nicholson and Phillips, 1981). $T2$ or spin–spin relaxation time is dependent on the frequency heterogeneity of the molecular microenvironment in which the water protons are embedded following a 90° RF pulse used in spin–echo (Fullerton, 1992; Wehrli, 1992). The more homogeneous the spin frequencies are to the water proton spin frequency then the longer the $T2$ relaxation times; conversely, the more out-of-phase the environmental spin frequencies to the spin–spin frequencies of the water protons then the shorter the $T2$ relaxation time. Shorter $T2$ relaxation times are present in the myelin, in comparison to the cytoplasm, because fat molecules (e.g., cholesterol (Konig, 1991) exhibit very different spin frequencies than water protons, thus creating a more heterogeneous spin–spin microenvironment. In contrast, longer $T2$ relaxation times are present in the cytoplasm and CSF because of a larger concentration of water molecules and thus a more homogeneous spin–spin microenvironment (Fullerton, 1992; Wehrli, 1992; Bottomley *et al.,* 1984).

In a previous study the relationship between $T2$ relaxation time of brain gray and white matter and EEG amplitude was evaluated in closed head injured (CHI) patients in which gray matter $T2$ relaxation time was related to decreased high frequency amplitude and white matter $T2$ relaxation time was related to increased low frequency amplitude (Thatcher *et al.,* 1998). The purpose of the present paper is to extend the previous analyses between nuclear magnetic resonance measures of cortical water proton relaxation times and

1053-8119/98 $25.00

EEG amplitude to measures of EEG coherence in CHI patients.

EEG coherence is a measure of "phase synchrony" or shared activity between spatially distant generators (Otnes and Enochson, 1972; Bendat and Piersol, 1980; Nunez, 1981). In the present study, EEG coherence will be analyzed using similar methods as previously published in which the spatial heterogeneity of scalp recorded EEG coherence is measured along two parallel lines with scalp electrodes equally spaced in the anterior-to-posterior and posterior-to-anterior directions (Thatcher *et al.,* 1986). This method of EEG coherence measurement is a normalization procedure in which all electrode reference and analysis procedures are experimentally analyzed as a function of interelectrode direction, interelectrode distance, and EEG frequency. Inflation of EEG coherence by reference electrodes was controlled in the present study (Fein *et al.,* 1988; Rappelsberger, 1989; Nunez *et al.,* 1997) because a single ear reference was held constant while electrode direction, distance, and frequency were systematically evaluated. This method of EEG coherence measurement is also a direct test of a two compartmental model of EEG coherence in which dynamic differences and interactions between short distance interelectrode distances (e.g., 7 cm) versus long interelectrode distances (e.g., 28 cm) have been measured (Thatcher *et al.,* 1986; 1987; Thatcher, 1992, 1994, 1998; Pascual-Marqui *et al.,* 1988; Nunez, 1981, 1994; van Baal, 1997). A second and more specific goal of the present paper is to compare and evaluate short- versus long-distance EEG coherence measures as they relate to $T2$ relaxation times of the protein/lipid membranes of the cortical gray and white matter.

2. METHODS

2.1 Closed Head Injured Patients

Two independent groups of CHI patients were studied. The first group of CHI patients was located at the James A. Haley VA Medical Center in Tampa, Florida (18 males and 1 female that ranged in age from 19 to 48 years; mean age = 32.6 years, SD = 10.6). This group of patients referred to as the "test" group was compared to an independent group of 21 CHI patients located at the Balboa Naval Medical Center in San Diego California (20 males and 1 female that ranged in age from 19 to 47 years, mean age = 25.33 years, SD = 7.43). This second group of CHI patients is referred to as the "replication" group. The patients in the test and replication groups were similar, having only closed traumatic brain injuries and a range of severity from mild to severe and whom were tested during the post acute to chronic period following injury (time from injury to EEG and MRI evaluation ranged from 10 days to 11 years with a mean of 1.7 years in the Tampa CHI group and from 11 days to 3.94 years with a mean of 257 days in the San Diego group between injury and EEG/MRI test), in which all of the patients were in the chronic or nonacute postinjury edema condition. Severity of injury varied from moderate to severe, but all of the subjects were conscious and alert with varying amounts of completed rehabilitation at the time of testing. The patients were tested as part of a multicenter Defense and Veterans Head Injury Program (DVHIP). All of the subjects were diagnosed using ICD-9 (i.e., Intracranial Injury excluding those with penetrating head wounds or codes within the 850 to 854 categories). Approximately 64% of the subjects were motor-vehicle accident (MVA) victims, 16% were victims of industrial or home accidents, and 20% were victims of violent crime.

2.2 Normal Control Subjects

A total of 12 male Neurologically normal high school students, ranging in age from 13.96 to 17.68 years (mean = 15.79 years; SD = 1.24 years), were also included in this study. The control subjects were recruited from local high schools in the San Diego area as part of a DVHIP pilot project to study the effects of football concussions on cognitive and neurological function (Daniel *et al.,* 1997). The MRI and EEG data included in the control subjects were obtained during the preseason period, prior to the football season.

2.3 EEG Recording

Power spectral analyses were performed on 2- to 5-min segments of eyes closed resting EEG recorded from 16 scalp locations using the left ear lobe as a reference. EKG and eye movement electrodes were applied to monitor artifact and all EEG records were edited to remove any visible artifact. The amplifier bandwidths were nominally 0.5 to 30 Hz, the outputs being 3 db down at these frequencies. Three to five minutes of eyes closed EEG was digitized at 100 Hz and then spectral analyzed using a complex demodulation procedure. Absolute EEG amplitude was computed from the 16 scalp locations in the delta (0.5 to 3.5 Hz), theta (3.5 to 7 Hz), alpha (7.5 to 13 Hz), and beta (13 to 22 Hz) frequency bands. The frequency bands, including the center frequencies (f_c) and one-half power values (B) were delta (0.5 to 3.5 Hz; $f_c = 2.0$ Hz; and $B = 1.0$), theta (3.5 to 7.0 Hz; $f_c = 4.25$ Hz; and $B = 3.5$ Hz), alpha (7.0 to 13.0 Hz; $f_c = 9.0$ Hz; and $B = 6.0$ Hz), beta (13 to 22 Hz; $f_c = 19$ Hz; and $B = 14.0$ Hz). EEG amplitude was computed as the square root of power.

EEG coherence and phase were computed for all pairwise combinations of electrodes (Otnes and Enochson, 1972; Thatcher *et al.,* 1986, 1989). Coherence is defined as

$$\Gamma^2_{xy}(f) = \frac{(G_{xy}(f))^2}{(G_{xx}(f)G_{yy}(f))}$$

where $G_{xy}(f)$ is the cross-power spectral density and $G_{xx}(f)$ and $G_{yy}(f)$ are the respective autopower spectral densities. Coherence was computed for all pairwise combinations of the following 16 channels (O1, O2, P3, P4, T5, T6, T3, T4, C3, C4, F3, F4, F7, F8, Fp1, Fp2), for each of the four frequency bands. The computational procedure to obtain coherence involved first computing the power spectra for x and y and then computing the normalized cross-spectra. Since complex analyses are involved this produced the cospectrum ("r" for real) and quadspectrum ("q" for imaginary). Then coherence was computed as:

$$\Gamma^2_{xy} = \frac{r^2_{xy} + q^2_{xy}}{G_{xx}G_{yy}}.$$

Further mathematical details of the analyses are provided in Thatcher *et al.* (1986, 1989).

The spatial heterogeneity of EEG coherence was assessed by measuring EEG coherence relations to $T2$ relaxation times along two parallel lines of scalp electrodes as shown in Fig. 1. The mean separation distance between adjacent electrode pairs was calculated to be 6.83 cm (or approximately 7 cm). This value was calculated by computing the mean inion to nasion distance for the population of 19 subjects and multiplying by 0.2 in order to approximate the average 10/20 electrode distance (Jasper, 1958), or u = (34.15 cm) (0.2) = 6.83 cm. In this way differences in the correlation between EEG coherence and $T2$ relaxation times in left versus right hemispheres and between short- and long-distance interelectrode distances was evaluated (Thatcher *et al.,* 1986).

2.4 MRI Acquisition

MR images were acquired within 1 to 4 days of the time that the scalp EEGs were recorded. For the Tampa VA group (N = 19), the MR images were acquired using a Picker 1.5T scanner with a double-spin echo for $T2$ and proton density and a $T1$-weighted spin-echo sequence. All acquisitions were precisely the same for all subjects and used 3-mm slices with no gaps between slices. The double echo proton density (PD) and $T2$ sequences were interleaved and had a TR = 3000 ms with TEs of 30 and 90 ms, FOV of 24 cm, a 90° flip angle and a 256 × 192 matrix. The $T1$-weighted sequence used TR = 883 ms with a TE = 20 ms, FOV = 24 cm, a 90° flip angle and a 256 × 192 matrix.

For the San Diego CHI group (N = 21) the MRI acquisition parameters were similar to that used in the Tampa CHI patients, i.e., the double echo PD and $T2$ sequences were interleaved and had a TR = 3000 ms with TE = 30 ms for PD and TE = 80 ms for 6 subjects and TE = 90 ms for 15 subjects. The $T1$-weighted sequence used TR = 883 ms for 6 subjects and a TR = 600 ms for 15 subjects with a TE = 20 ms. All of the San Diego acquisitions had a FOV = 24 cm, a 90° flip angle and a 25 × 192 matrix. The quantitative EEGs were acquired using amplifiers with the same filter and gain settings and the same EEG analysis procedures for the calculation of EEG coherence were used as described in section 2.3.

For the normal control group (N = 12) the MRI acquisition parameters were similar to that used in the Tampa and San Diego CHI patients, i.e., the double echo PD and $T2$ sequences were interleaved with a TR = 4000 ms and TE = 15 ms for PD and TE = 90 ms for $T2$. The $T1$-weighted sequence used TR = 550 ms for 15 subjects with a TE = 20 ms. All of the normal control acquisitions had a FOV = 24 cm, a 90° flip angle and a 256 × 192 matrix. The quantitative EEGs were acquired using the same amplifiers with the same filter and gain settings and the same EEG analysis procedures for the calculation of EEG coherence as described in section 2.3.

2.5 Segmentation and Slice Selection

A multispectral (i.e., $T1$, $T2$, and PD) k-nearest neighbor (kNN) manual segmentation and classification algorithm and a multispectral fuzzy c-means (FCM) algorithm was used for gray matter, white matter, and CSF segmentation (Clarke *et al.,* 1994; Bezdek *et al.,* 1992; Bensaid *et al.,* 1994). This involved the use of a brain mask that was manually traced for each axial proton density image via a polygon-tracing algorithm isolating the brain from skull and dura. To minimize error and to improve segmentation accuracy a validity-guided reclustering (VGC) algorithm was used on each FCM-segmented slice (Bensaid *et al.,* 1994). Every segmented slice was manually classified via a graphical–user interface into five classes: background, white matter, gray matter, CSF, and other. Slice number 1 or the lowest starting slice was identified as being at the level of the genu of the corpus callosum, septum pellucidum, and the forceps major and minor. Slices 1 to 15 represent a contiguous spatial volume of 4.5 cm (i.e., 3 mm × 15 = 4.5 cm) beginning from the starting slice and extending to the top of the cortex (Thatcher *et al.,* 1997). Figure 1 illustrates the location and orientation of the slice volume in this study.

2.6 Calculations of ^{1}H NMR T2 Relaxation Times

We used the solutions of the Bloch equations (Bloch, 1946) to calculate T2 relaxation time (Dixon and Ekstrand, 1982; Kjos *et al.,* 1985; Darwin, 1986; Hickley, 1986; Mills *et al.,* 1984). According to this solution, MR signal intensity (I) is related to ^{1}H relaxation times by: $I = KN(1 - e^{-TR/T1})e^{-TE/T2}$, where K = velocity and scaling constants, N = hydrogen spin density, TR = repetition time, TE = echo time, $T1$ = spin–lattice

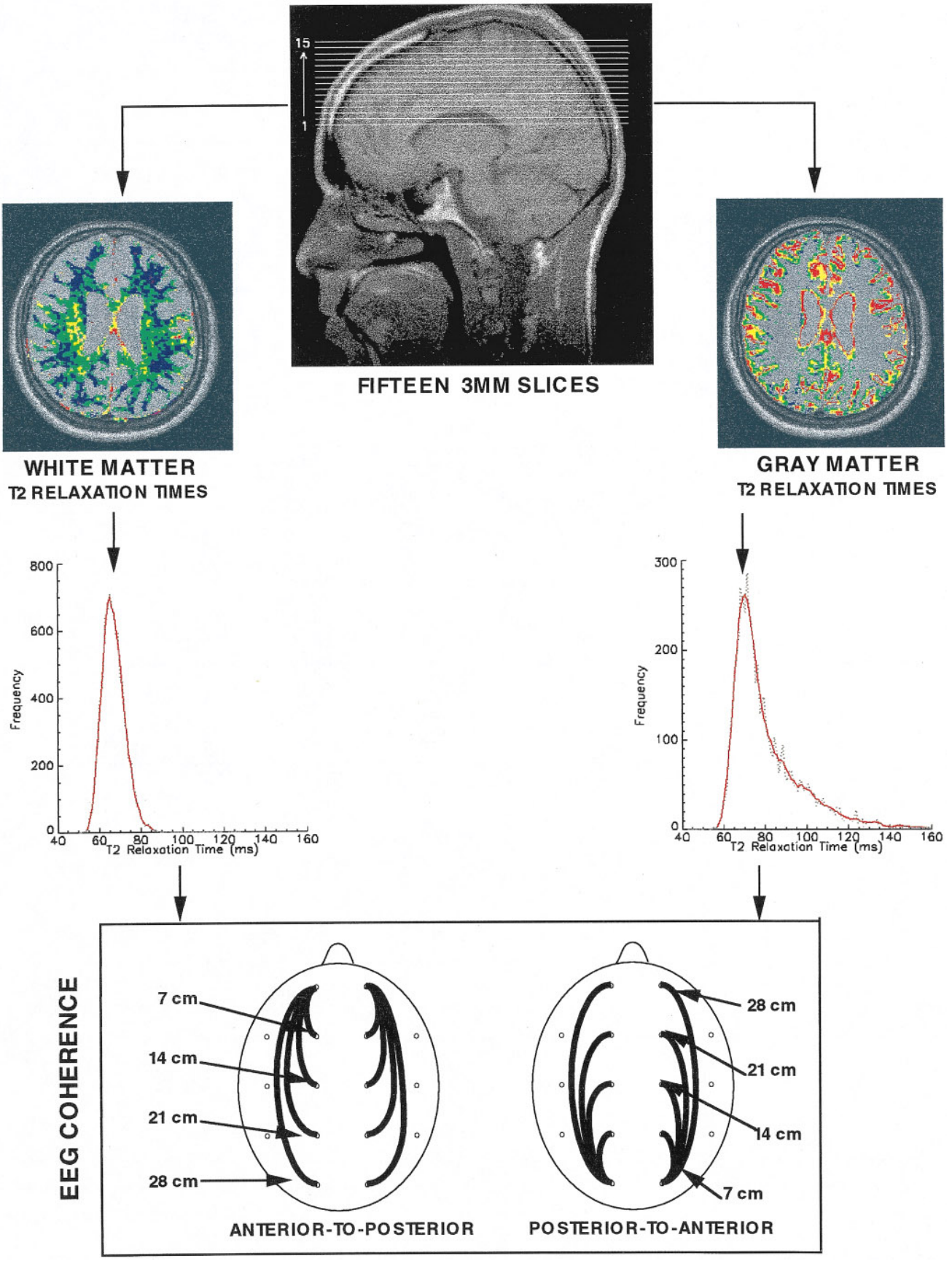
15
1
FIFTEEN 3MM SLICES
WHITE MATTER
T2 RELAXATION TIMES
GRAY MATTER
T2 RELAXATION TIMES
Frequency
T2 Relaxation Time (ms)
Frequency
T2 Relaxation Time (ms)
EEG COHERENCE
7 cm
14 cm
21 cm
28 cm
ANTERIOR-TO-POSTERIOR
28 cm
21 cm
14 cm
7 cm
POSTERIOR-TO-ANTERIOR

relaxation time, and $T2$ = spin–spin relaxation time. $T2$ was solved analytically using the PD and $T2$ images acquired in an interleaved manner where the corresponding TR values were equal, $TR \gg TE$ and molecular velocity and scaling = 1. The equation was

$$T2 = \frac{TE_{PD} - TE_{T2}}{\ln (I_{T2}/I_{PD})}$$

where I_{T2} and I_{PD} were the pixel intensities from the respective $T2$ and PD images (mathematical details are provided in Appendix A).

The $T2$ gray matter and white matter histogram distributions within a given 3-mm slice were always unimodal but sometimes skewed or kurtotic (Thatcher *et al.,* 1997). The rationale for the use of the mode, in contrast to the mean, is that the mode represents the most frequently occurring value within a sample. Errors in segmentation, which primarily occur at the boarders of tissue classes, are minimized by the use of the mode. Thus, in order to use a reliable and simple measure the frequency histogram was first smoothed using a 4th order Savitzky and Golay (1964) procedure (see Thatcher *et al.,* 1997, 1998, for further details) and then the mode of the frequency distribution of T2 for the segmented gray matter and white matter was calculated for each axial slice and used as the MRI-independent variable in this study.

Figure 1 shows the experimental design in which 15 3-mm MRI slices were segmented into gray and white matter and then the mode of $T2$ relaxation time for each slice was calculated in milliseconds. Both the whole modes of $T2$ relaxation time as well as individual slice mode of $T2$ relaxation times were then related by analyses of variance and correlation to EEG coherence recorded in the anterior-to-posterior and posterior-to-anterior directions and at different interelectrode distances as shown in the bottom of Fig. 1.

3. RESULTS

3.1 Multivariate Analyses of Variance in the Tampa "Test" Population

A multivariate analysis of variance (MANOVA) was conducted on the Fischer transformed correlation matrix of gray and white matter $T2$ relaxation times for the 15 slices and EEG coherence in the four frequency bands at 7-, 14-, 21-, and 28-cm interelectrode distances (Velleman, 1995; Cohen and Cohen, 1983). Separate MANOVAs were conducted for the whole volume $T2$ relaxation of gray matter and white matter. The overall main effect of EEG frequency was statistically significant in the gray matter $T2$ relaxation ($df = 3, F = 15.21$, $P < .0001$) but it was not statistically significant for the white matter $T2$ relaxation ($df = 3, F = 2.3, P = .0869$). The overall main effect of interelectrode distance was statistically significant for both gray matter $T2$ relaxation ($df = 3$, $F = 22.796$, $P < 0.0001$) and white matter $T2$ relaxation ($df = 3$, $F = 9.02$, $P < 0.0001$) with only the shortest (7 cm) and the longest (28 cm) interelectrode distances being statistically significant. The overall main effect of electrode direction (i.e., anterior-to-posterior versus posterior-to-anterior) was not statistically significant for the gray matter $T2$ relaxation time ($df = 1$, $F = 0.0661$, $P = 0.798$), but direction was statistically significant for the white matter $T2$ relaxation time ($df = 1$, $F = 23.946$, $P < 0.0001$), with only the anterior-to-posterior direction being statistically significant. Finally, the overall main effect for EEG coherence recorded from the left versus right hemisphere was not statistically significant for either the gray matter $T2$ relaxation time ($df = 1$, $F = 0.907$, $P = 0.345$) or for the white matter $T2$ relaxation time ($df = 1, F = 0.055, P = 0.8154$).

Differences in gray matter $T2$ relaxation and EEG coherence versus white matter $T2$ relaxation and EEG coherence were evaluated with MANOVA in which the dependent variables were the EEG coherence measures of frequency, direction, hemisphere, and distance and the factors were $T2$ gray relaxation and $T2$ white matter relaxation. A significant main effect was present in the alpha frequency band ($df = 1, F = 5.41, P < 0.02$), where gray matter $T2$ was more highly correlated with a decrease in EEG alpha coherence than white matter $T2$. A significant main effect of direction was present ($df = 1, F = 13.151, P < 0.0006$) where gray matter $T2$ was more highly correlated with EEG coherence than white matter $T2$ in the anterior-to-posterior direction. No statistically significant differences between gray and white matter $T2$ were present in the posterior-to-anterior direction. Finally, gray matter $T2$ was more

FIG. 1. Diagram of the MRI and EEG experimental design. Top center shows the location of the 15 3-mm MRI slices (Thatcher *et al.,* 1997, 1998). Top left and right are examples of T2 relaxation time maps from the segmented white and gray matter showing the distribution of T2 relaxation times in a given slice. T2 relaxation time is represented in pseudocolor where blue = 45–60 ms, green = 60–75 ms, yellow = 75–90 ms, orange = 90–105 ms, and red = 105–120 ms. Middle row is the T2 relaxation time histograms from the segmented white matter (left) and gray matter (right). The dots are the actual T2 values and the solid line is the Savitzky and Golay (1964) fit of the distributions. The mode of the smoothed T2 histogram for each axial slice was the independent variable in this study. Methods of computing T2 relaxation times from a conventional MR image are described in the text and Appendix A. The bottom row shows the location of the scalp electrodes for the purposes of computing left and right hemisphere and anterior-to-posterior and posterior-to-anterior directions of EEG coherence. Both the short (i.e., approx. 7-cm adjacent electrodes), intermediate (e.g., 14 cm), and long distance interelectrode distances (e.g., 21 and 28 cm) are also shown at the bottom of the figure.

TABLE 1

Gray Matter: Manova *t*-Ratios for EEG Coherence and Gray Matter T2 Relaxation Times in the Ant-to-Post and Post-to-Ant Directions

	7 cm		14 cm		21 cm		28 cm	
	L	R	L	R	L	R	L	R
A-P								
Delta	−8.88***	−23.7***	—	—	4.57**	11.84***	4.34**	11.72***
Theta	−5.49**	−5.7**	—	—	—	—	6.15***	4.55**
Alpha	—	−5.24**	—	−3.9**	—	—	3.39*	9.58***
Beta	—	—	—	−5.06**	—	2.8*	—	3.02*
P-A								
Delta	−7.73**	−10.3***	—	—	3.25*	4.48**	3.12*	7.27**
Theta	—	−4.79**	—	—	—	2.62*	3.02*	4.26**
Alpha	—	−3.99*	—	—	—	—	3.5*	4.0*
Beta	—	−2.72*	—	—	—	—	—	—

Note. * $P < .05$; ** $P < .005$; *** $P < .0005$.

highly correlated with short distance (7 cm) EEG coherence measures ($df = 1$, $F = 5.45$, $P < 0.03$) than white matter $T2$.

A summary of the number and sign of statistically significant Bonferroni adjusted relations between $T2$ relaxation time and EEG coherence in the delta, theta, alpha, and beta frequency bands for the electrode pairings is shown in Tables 1 and 2. Importantly, the sign of the t tests in Tables 1 and 2 is reversed for the 7-cm interelectrode distance as compared to the 28-cm interelectrode distances. That is, lengthened $T2$ in both the gray and white matter is related to a decrease in EEG coherence in the 7-cm or short interelectrode distances but is positively related to EEG coherence in the long interelectrode distances (i.e., 28 cm). It can also be seen in Tables 1 and 2 that there are more and stronger statistically significant relations in the lower frequency bands (e.g., delta and theta) than in the higher frequency bands (e.g., beta).

3.2 Correlations between Individual Slice T2 Relaxation Times and EEG

Figure 2 shows examples of the scattergram plots of the relationships between $T2$ relaxation times and EEG coherence represented in Tables 1 and 2 and Figs. 3 and 4. The left column is relations between $T2$ relaxation time and long interelectrode distances (28 cm) and the right column is relations between $T2$ relaxation time and short interelectrode distances (7 cm). Consistent with Tables 1 and 2, differences in the polarity or direction of correlation between long (28 cm) versus short (7 cm) interelectrode distances in the anterior-to-posterior and posterior-to-anterior directions were frequently present.

TABLE 2

White Matter: Manova *t*-Ratios for EEG Coherence and White Matter T2 Relaxation Times in the Ant-to-Post and Post-to-Ant Directions

	7 cm		14 cm		21 cm		28 cm	
	L	R	L	R	L	R	L	R
A-P								
Delta	—	−3.2*	—	—	—	—	—	2.67*
Theta	−4.17**	−3.5*	—	—	—	—	6.37**	5.33**
Alpha	—	−3.75*	—	—	—	—	—	7.89***
Beta	—	—	—	−11.4***	—	3.37*	−2.79*	8.08***
P-A								
Delta	−4.69**	−10.2***	—	−3.13*	—	2.97*	4.86**	10.32***
Theta	—	−4.97**	−4.86**	−4.01*	—	—	8.74***	7.73***
Alpha	−2.77*	−5.83**	−4.43**	−6.01**	3.33*	5.26**	3.87*	6.58**
Beta	—	−3.69*	—	−4.34**	—	—	—	6.67***

Note. * $P < .05$; ** $P < .005$; *** $P < .0005$.

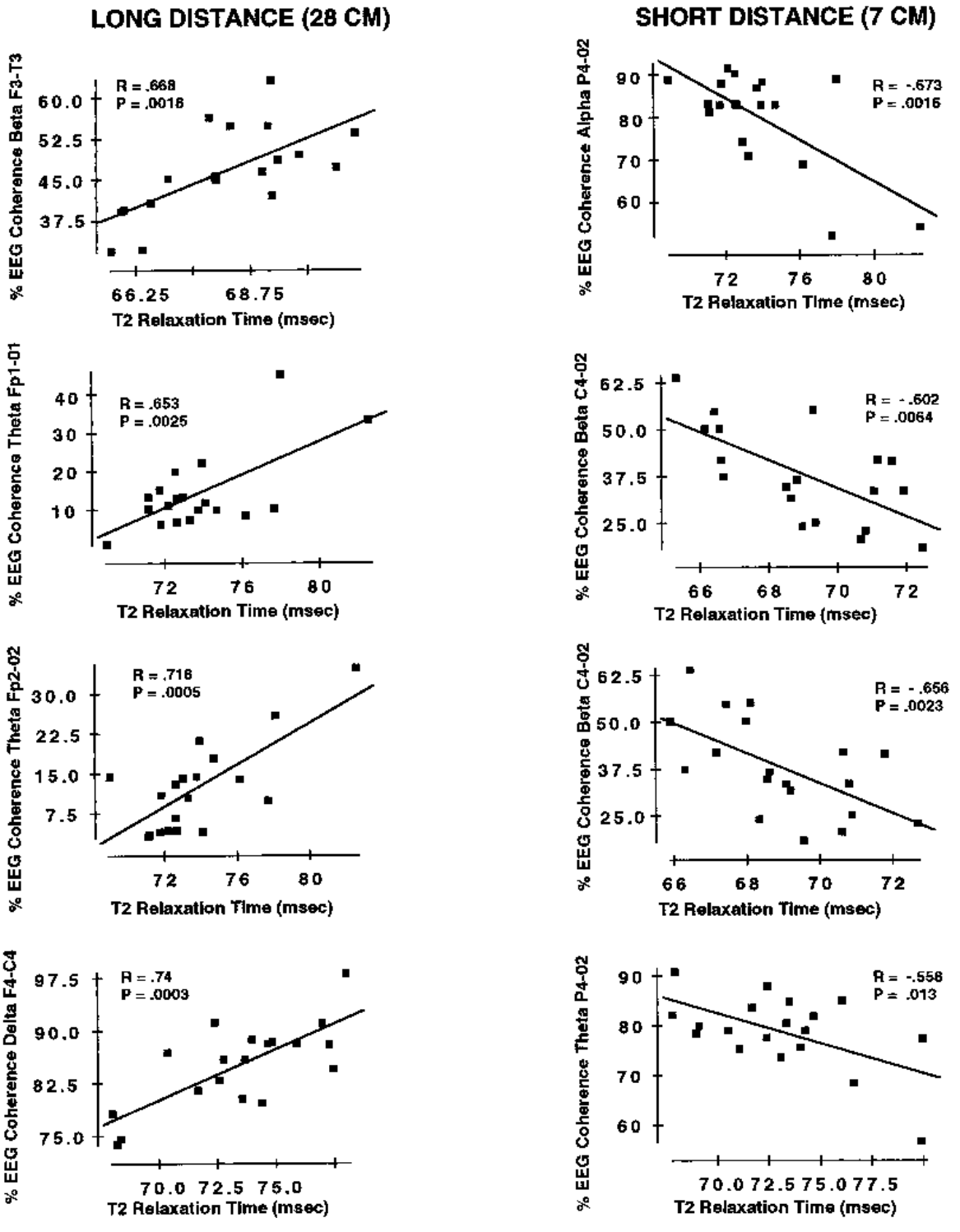

FIG. 2. T2 and EEG coherence scattergrams. Representative scattergrams between T2 relaxation time (x-axis) and EEG coherence (y-axis). The left column are scattergrams from long EEG interelectrode distances (28 cm) and the right column are scattergrams from short distance EEG interelectrode distances (7 cm). Opposite directions of correlation are evident in the short versus the long interelectrode distances in which as T2 lengthens then short distance EEG coherence declines and long distance EEG coherence increases. *R* is the correlation coefficient and *P* is the exact two-tail probability value.

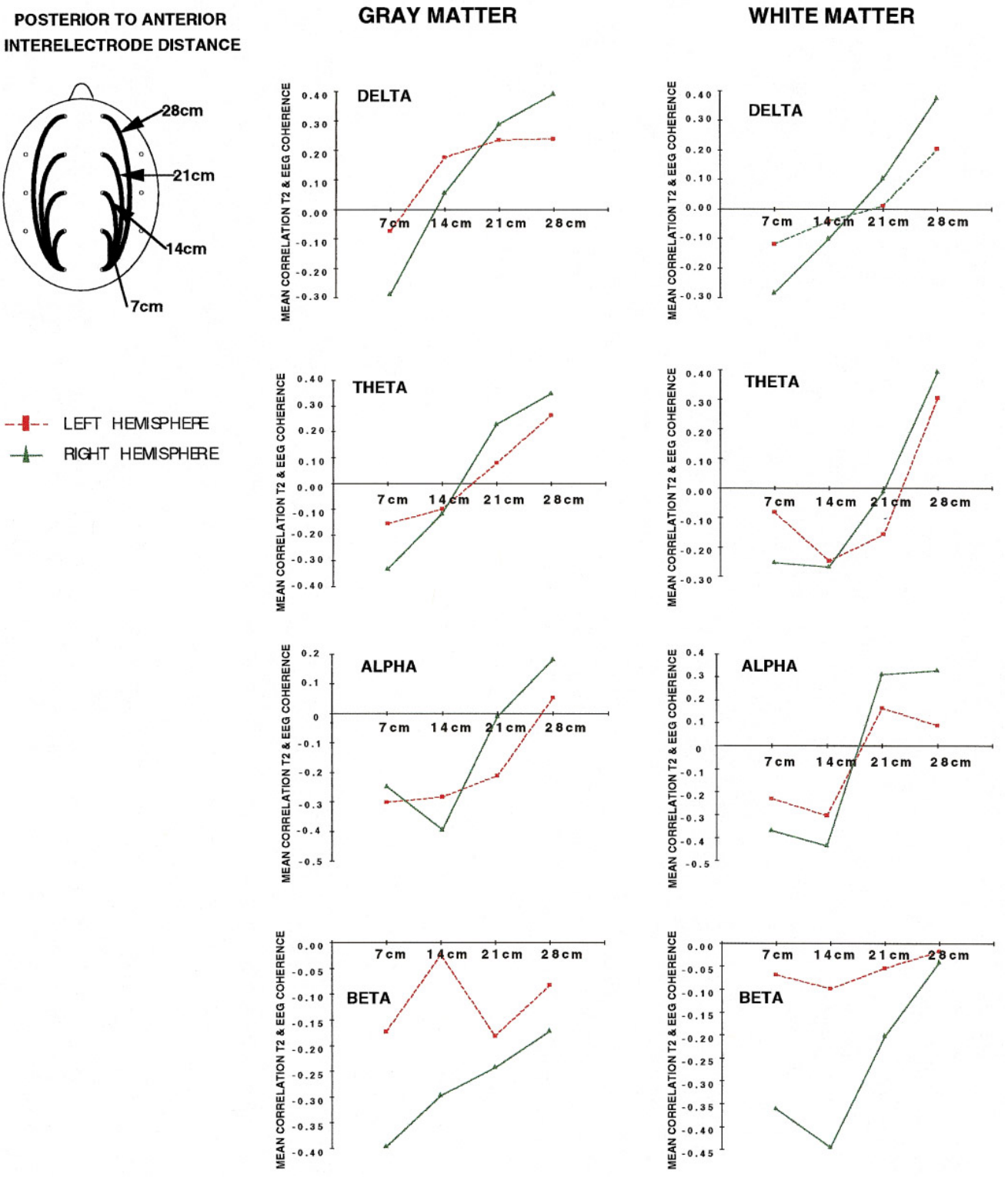

FIG. 3. Mean correlations between T2 relaxation time and EEG coherence in the posterior-to-anterior direction. An illustration of the posterior-to-anterior electrode arrangement is shown at the top left. The left column are mean correlations between gray matter T2 relaxation time and EEG coherence and the right column are mean correlations between white matter T2 relaxation time and EEG coherence. The mean correlation is the average correlation between T2 relaxation time and EEG coherence for all 15 MRI slices (i.e., a 4.5-cm volume). Comparisons in mean correlation for the four different interelectrode distances (i.e., 7, 14, 21, and 28 cm) are shown on the x-axis. In general, negative correlations between T2 and EEG coherence are present in the short interelectrode distances while positive correlations tend to be present in the long interelectrode distances, especially in the delta and theta frequency bands. The beta frequency band failed to reveal a similar polarity reversal as a function of interelectrode distance.

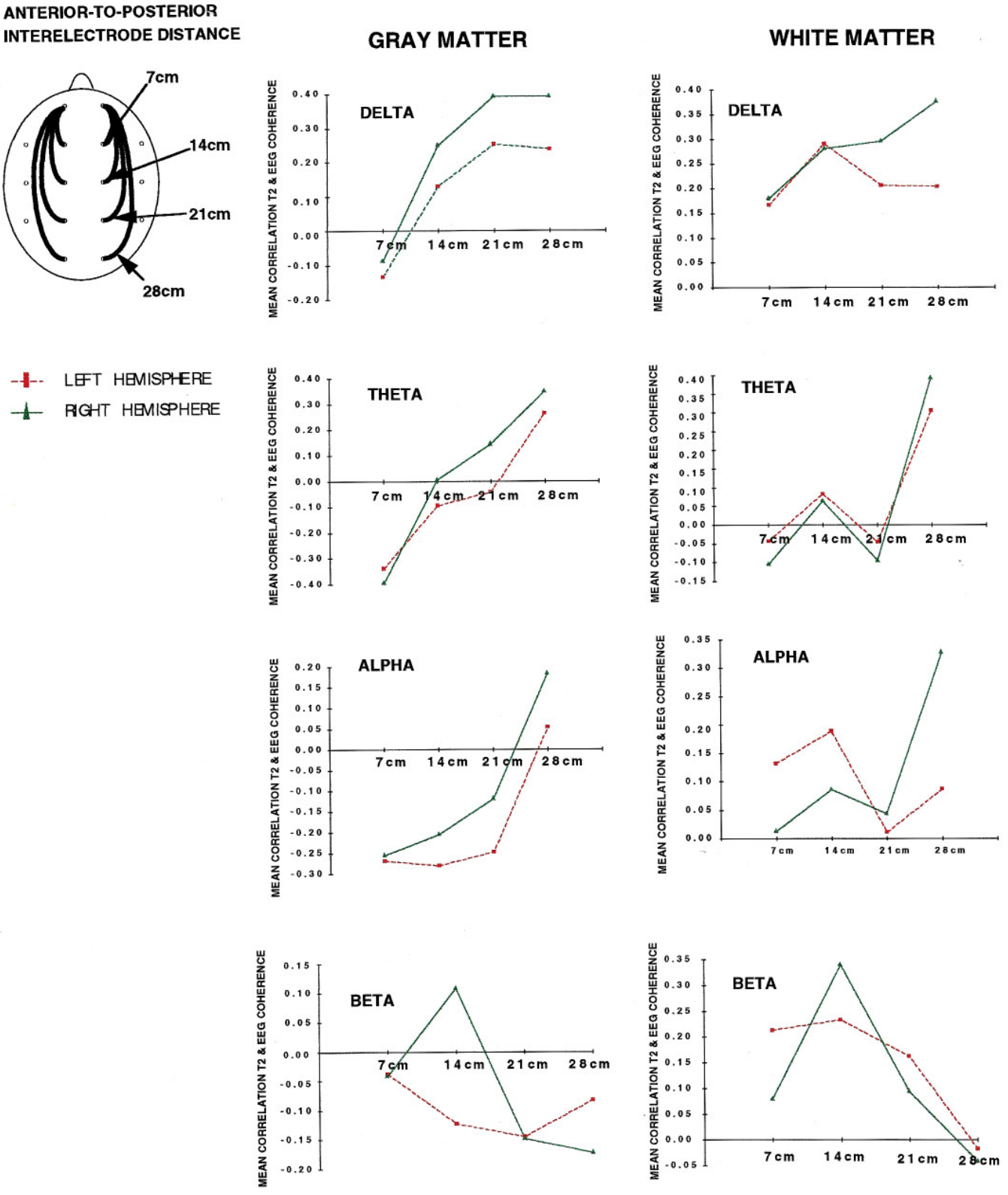

FIG. 4. Mean correlations between T2 relaxation time and EEG coherence in the anterior-to-posterior direction. An illustration of the anterior-to-posterior electrode arrangement is shown at the top left. The left column are mean correlations between gray matter T2 relaxation time and EEG coherence and the right column are mean correlations between white matter T2 relaxation time and EEG coherence. The mean correlation is the average correlation between T2 relaxation time and EEG coherence for all 15 MRI slices (i.e., a 4.5-cm volume). Comparisons in mean correlation for the four different interelectrode distances (i.e., 7, 14, 21, and 28 cm) are shown on the x-axis. In the gray matter negative correlations between T2 and EEG coherence are present in the short interelectrode distances while positive correlations tend to be present in the long interelectrode distances, especially in the delta and theta frequency bands. The beta frequency band failed to reveal a similar polarity reversal as a function of interelectrode distance.

3.3 Mean Correlations between Whole Volume T2 Relaxation Times and EEG Coherence

Figure 3 shows the whole volume or the mean of the 15 slice correlations between $T2$ relaxation time and EEG coherence at different interelectrode distances in the left and right hemisphere in the posterior-to-anterior direction for the different EEG frequency bands. A similar profile of correlation versus EEG frequency was observed in both the gray matter and white matter $T2$ relaxation time, namely, a negative correlation with short interelectrode distances (e.g., 7 cm) but a positive correlation with long interelectrode distances (e.g., 28 cm). The polarity reversal in correlation between short versus long distances was strongest in the delta and theta bands and weakest in the beta frequency band, with the alpha frequency band somewhat intermediate.

Figure 4 shows the mean correlation between $T2$ relaxation time and EEG coherence at different interelectrode distances in the left and right hemisphere in the anterior-to-posterior direction for the different EEG frequency bands. Similar to the posterior-to-anterior direction in Fig. 3, difference in the polarity of correlation to lengthened $T2$ for short versus long interelectrode distances was observed in both the gray matter and white matter with short interelectrode distances (e.g., 7 cm) negatively correlated to lengthened $T2$ relaxation time and long interelectrode distances (e.g., 28 cm) positively correlated to lengthened $T2$ relaxation time. The polarity difference in correlation between short versus long distances was strongest in the delta and theta bands and weakest in the beta frequency band. The correlations between $T2$ relaxation time and the beta frequency band were all negative with stronger negative correlations in the short-distance (7 cm) and nearly zero correlation in the long-distance connections (28 cm). The beta frequency band also exhibited the strongest differences in correlation polarity in the anterior-to-posterior direction (Fig. 4) versus the posterior-to-anterior direction (Fig. 3).

3.4 Independent Replication of T2 Relaxation Time and EEG Coherence Correlations

It is important to assess the replicability and generality of the observed relationship between $T2$ relaxation time and EEG coherence in an independent population of patients. Therefore, EEG coherence and $T2$ relaxation times were measured from an independent population of 21 CHI patients whose MRI and EEG were acquired using a different MRI scanner (e.g., a Siemen's 1.5T scanner) and from a different location and different EEG technicians (e.g., Balboa Naval Medical Center in San Diego).

Figure 5 shows the mean correlation between $T2$ relaxation time and EEG coherence at different interelectrode distances in the left and right hemisphere in the anterior-to-posterior direction for the different EEG frequency bands in the 21 San Diego CHI patients. A clear replication of the relationship between $T2$ and EEG coherence observed in the Tampa VA population of CHI patients (see Figs. 2 and 3) was also observed in the San Diego population. Specifically, the same difference in the polarity of correlation with $T2$ for short versus long interelectrode distances was observed in both the gray matter and white matter with short interelectrode distances (e.g., 7 cm) negatively correlated with $T2$ relaxation time and long interelectrode distances (e.g., 28 cm) positively correlated with $T2$ relaxation time. Similar to the Tampa VA population, the strongest polarity differences between short and long distances were in the lower frequency bands.

3.5 Correlations between EEG Coherence and Neuropsychological Functioning

An important issue is whether the observed correlations between $T2$ relaxation time and EEG coherence reflect a compensatory process or, instead, are a direct consequence of pathology. According to a pathology hypothesis, biomechanical damage results in a reduction in the fidelity and efficiency of short-distance cortical communication and increased long-distance cortical communication is due to reduced short-distance communication because of the competitive relationship between short- and long-distance connections. The opposite would be expected if a compensatory process were present. According to a compensatory hypothesis, decreased short-distance coherence reflects increased functional differentiation and increased long-distance coherence reflects increased integration, which facilitates cognitive functioning.

In order to test these hypotheses multivariate analysis of variance was conducted between EEG coherence and neuropsychological test scores on the Boston Naming Test, Digit Span Backward, Digit Span Forward, and the Wisconsin Card Sort Test. Separate MANOVAs were conducted for frontal short-distance (i.e., $F_{1/2}$–$F_{3/4}$) and long-distance interelectrode distances ($F_{1/2}$–$O_{1/2}$). The neuropsychological test scores were the dependent variables and EEG coherence in the delta, theta, alpha, and beta frequency bands were the factors. A statistically significant main effect of neuropsychological test performance was present for both short- and long-distance interelectrode distances. A summary of the multivariate F and P values from the MANOVA for the neuropsychological test scores and EEG coherence is shown in Table 3.

Figure 6 shows the mean correlations between different interelectrode distances of EEG coherence and cognitive function. Short-distance coherence was always positively related to cognitive performance, especially in the higher frequency bands. Long-distance

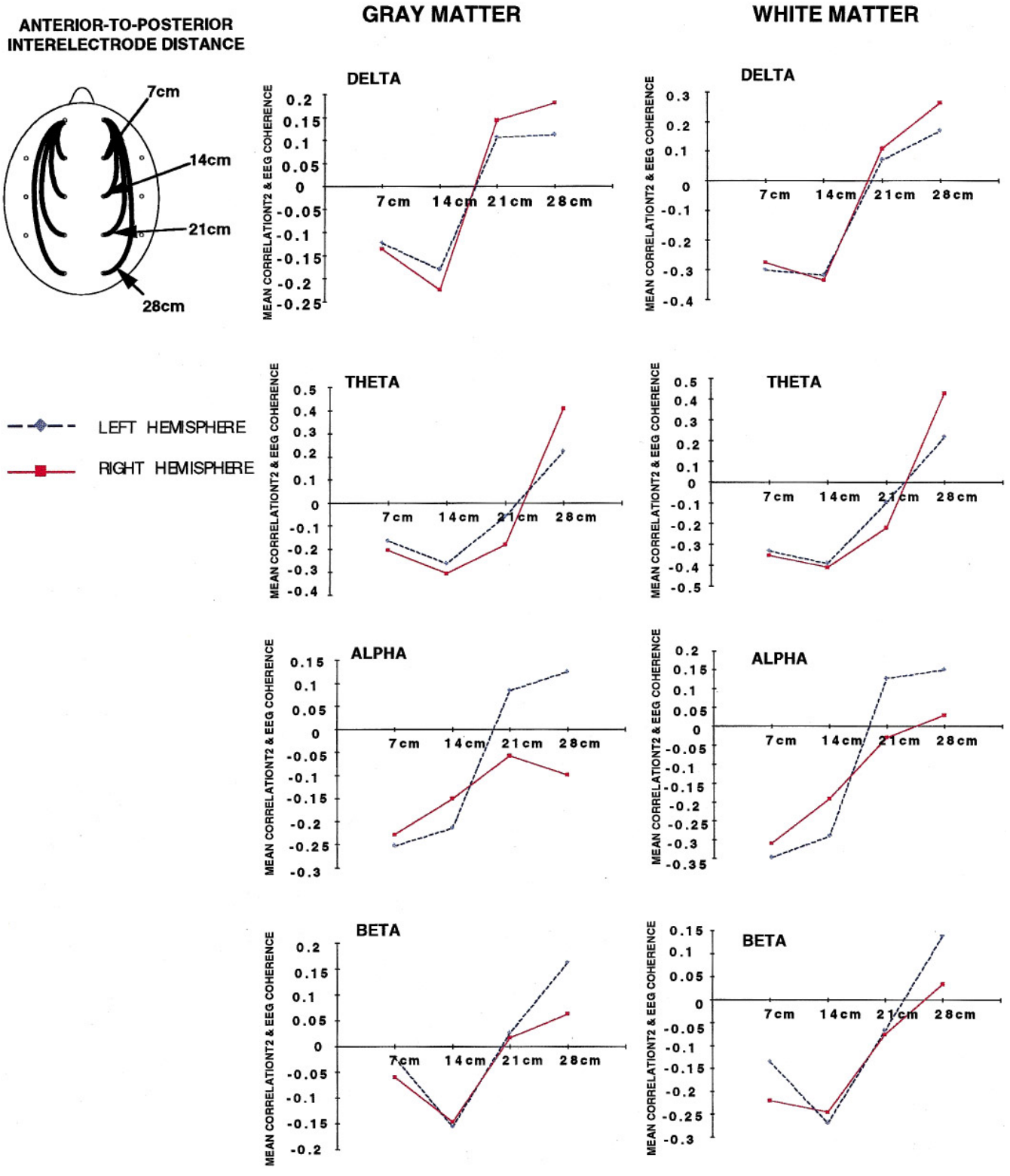

FIG. 5. Independent replication of T2 relaxation time and EEG coherence correlations. The left column are mean correlations between gray matter T2 relaxation time and EEG coherence and the right column are mean correlations between white matter T2 relaxation time and EEG coherence. The mean correlation is the average correlation between T2 relaxation time and EEG coherence for all 15 MRI slices (i.e., a 4.5-cm volume). Comparisons in mean correlation for the four different interelectrode distances (i.e., 7, 14, 21, and 28 cm) are shown on the x-axis. Similar to Figs. 3 and 4, negative correlations between T2 and EEG coherence are present in the short interelectrode distances while positive correlations tend to be present in the long interelectrode distances, especially in the delta and theta frequency bands of the gray matter. This figure represents an independent replication of the polarity reversal between short and long interelectrode distances seen in Figs. 3 and 4.

TABLE 3

MANOVA Results for EEG Coherence and Neuropsychological Test Performance

	Wisconsin categories	Wisconsin total errors	Boston naming	Visual spatial learning
7 cm elect. distance	$F = 31.42$ $P = .0091$	$F = 31.86$ $P = .0004$	$F = 32.327$ $P = .0003$	$F = 16.177$ $P = .0234$
28 cm elec. distance	$F = 9.372$ $P = .0108$	NS	NS	$F = 34.449$ $P = .0001$

coherence, on the other hand, was either negatively correlated or had no significant positive correlation with cognition. These results support the direct consequence of injury hypothesis and not the compensatory hypothesis.

3.6 Mean Correlations between T2 Relaxation Times and EEG Coherence in Normal Subjects

The previous analyses have shown statistically significant correlations between *T*2 relaxation time and EEG coherence in patients with closed head injuries. However, it is unknown whether a similar relationship is present in correlations between *T*2 relaxation time and EEG coherence in normal subjects who do not have a history of traumatic brain injury. Therefore, a group of 12 normal volunteers were also studied.

Figure 7 shows the mean correlation between *T*2 relaxation time and EEG coherence at different interelectrode distances in the left and right hemisphere in the anterior-to-posterior direction for the different EEG frequency bands in the 12 Neurologically normal subjects. Unlike the Tampa and San Diego CHI patients, the normal subjects failed to exhibit a difference in the polarity of correlation with T2 for short versus long interelectrode distances in the delta, theta or alpha frequency bands. However, a clear polarity difference for *T*2 correlations with short- versus long-distance EEG coherence was present in the beta frequency band, especially from the left hemisphere. Figure 8 shows superimposed correlations between T2 relaxation time and EEG coherence in the anterior-to-posterior direction in the beta frequency band for all 15 MRI slices. A consistent difference in the polarity of correlation between T2 relaxation time and short distance (e.g., 7 to 14 cm) versus long distance (e.g., 21 to 28 cm) EEG coherence can be seen in both the white and gray matter analyses.

4. DISCUSSION

The results of this study demonstrated statistically significant relations between MRI-derived *T*2 relaxation times and electroencephalographic (EEG) coherence in which increased *T*2 relaxation times in both the cortical gray and white matter were related to: (1) decreased EEG coherence between short interelectrode distances (e.g., 7 cm) and increased EEG coherence between long interelectrode distances (e.g., 28 cm) and (2) differences in EEG frequency in which *T*2 relaxation time was most strongly related to the lower frequency bands in CHI patients and to the higher frequency band in normal controls. Differences between the gray matter *T*2 relaxation and white matter *T*2 relaxation were also observed in which the gray matter *T*2 was more strongly related to EEG coherence than the white matter *T*2 (see Tables 1 and 2). These effects were not correlated with the interval of time between injury and MRI test, nor with edema and acute injury effects (e.g., mean post injury time = 1.7 years). Most importantly, from an electrophysiological perspective, the reference electrode or other possible electrophysiological recording or analysis problems cannot explain differences in the short- vs long-distances, nor, the anterior-to-posterior and posterior-to-anterior directions of correlations, nor, the spectral frequency correlations observed in this study (Fein *et al.,* 1988; Rappelsberger, 1989; Nunez *et al.,* 1997). Finally, an independent replication of these findings was obtained in an independently obtained sample of 21 closed head injured patients (i.e., different geographic location and different MRI and EEG machines, see Fig. 5) and the short- versus long-distance pattern of correlation was also observed in Neurologically normal subjects (see Figs. 7 and 8).

These findings, when taken as a whole, indicate that changes in the biophysical properties of the protein/lipid microenvironment of the human brain are related to EEG coherence. The observed correlations clearly do not establish a causal linkage between *T*2 relaxation time and EEG coherence. However, they do give rise to hypotheses capable of explaining such a linkage and to the extent that the hypotheses are experimentally verified, then a biophysical linkage exists. If the hypotheses are experimentally rejected, then a nonbiophysical explanation of these findings will be established. It is in this context that experimentally explorable hypotheses will be suggested.

4.1 Two Compartmental Model of EEG Coherence and T2 Relaxation Time

On the basis of the fine structure of cortico-cortical connections, a two-compartmental model of cortico-cortical organization was suggested by Braitenberg (1978), demonstrating two distinct cortico-cortical fiber systems: (1) A gray matter or "Alpha" system which contains short distance cortico-cortical axons involved in local interactions on the order of millimeters to a few centimeters, which occur primarily within the gray matter, and (2) a white matter or "Beta" system, which contains long-distance axons that exit the gray matter

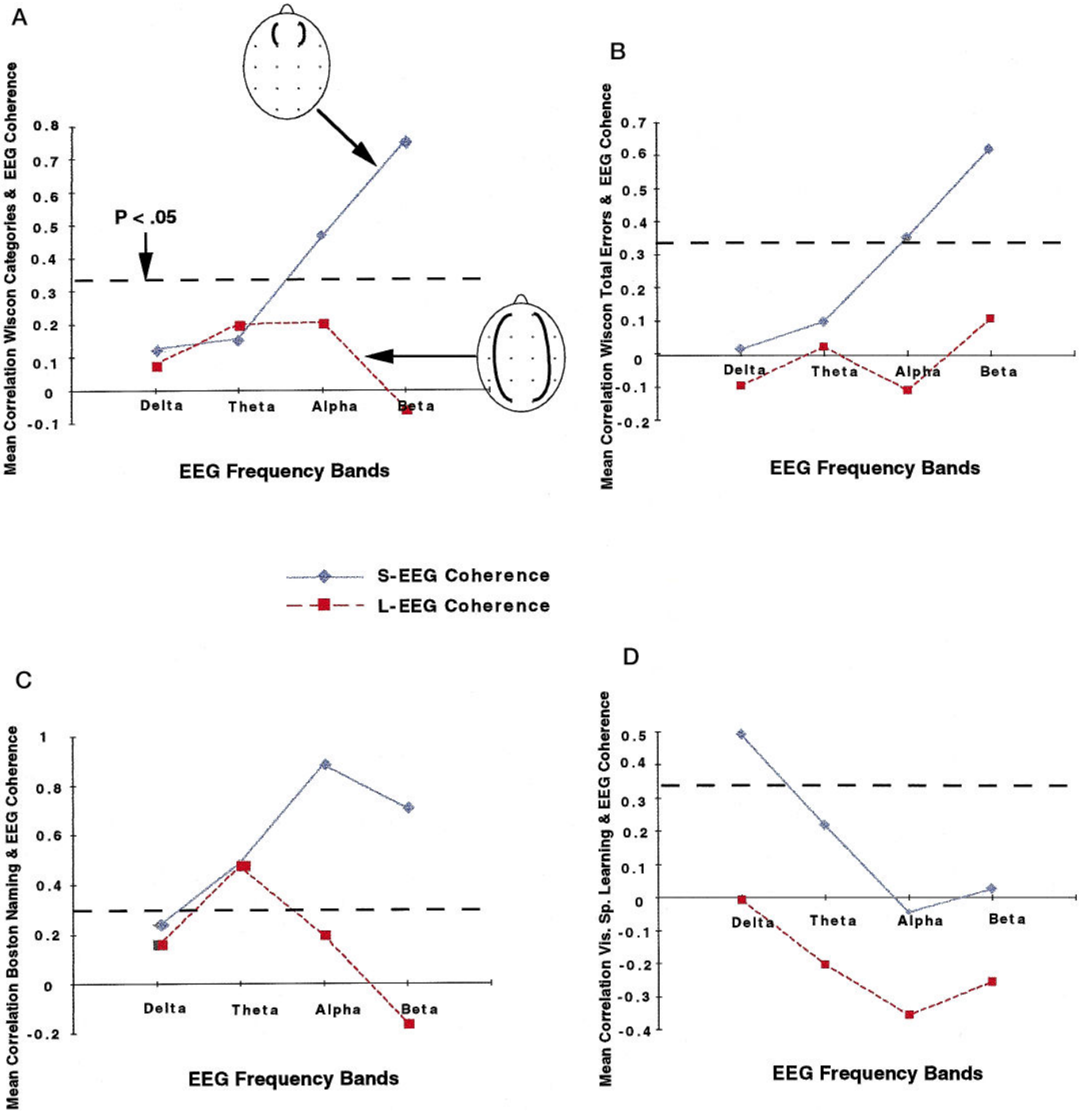

FIG. 6. Correlations between EEG coherence neuropsychological functioning. Mean correlations between different interelectrode distances of EEG coherence and cognitive function as measured by four different neuropsychological tests (A, B, C, and D). Mean correlation between cognitive function and short distance EEG coherence (7 cm, or S-EEG) is represented by the solid lines and long-distance EEG coherence (28 cm, or L-EEG) is represented by the dashed lines. EEG frequency is represented on the x-axis. Positive correlations between short distance EEG coherence and cognitive function was evident for all the neuropsychological tests (i.e., A, B, C, and D). That is, as EEG coherence increases between short interelectrode distances then cognitive performance increases. Long distance coherence was only weakly correlated to cognitive performance. Dashed line represents the univariate $P < 0.05$ level of statistical significance.

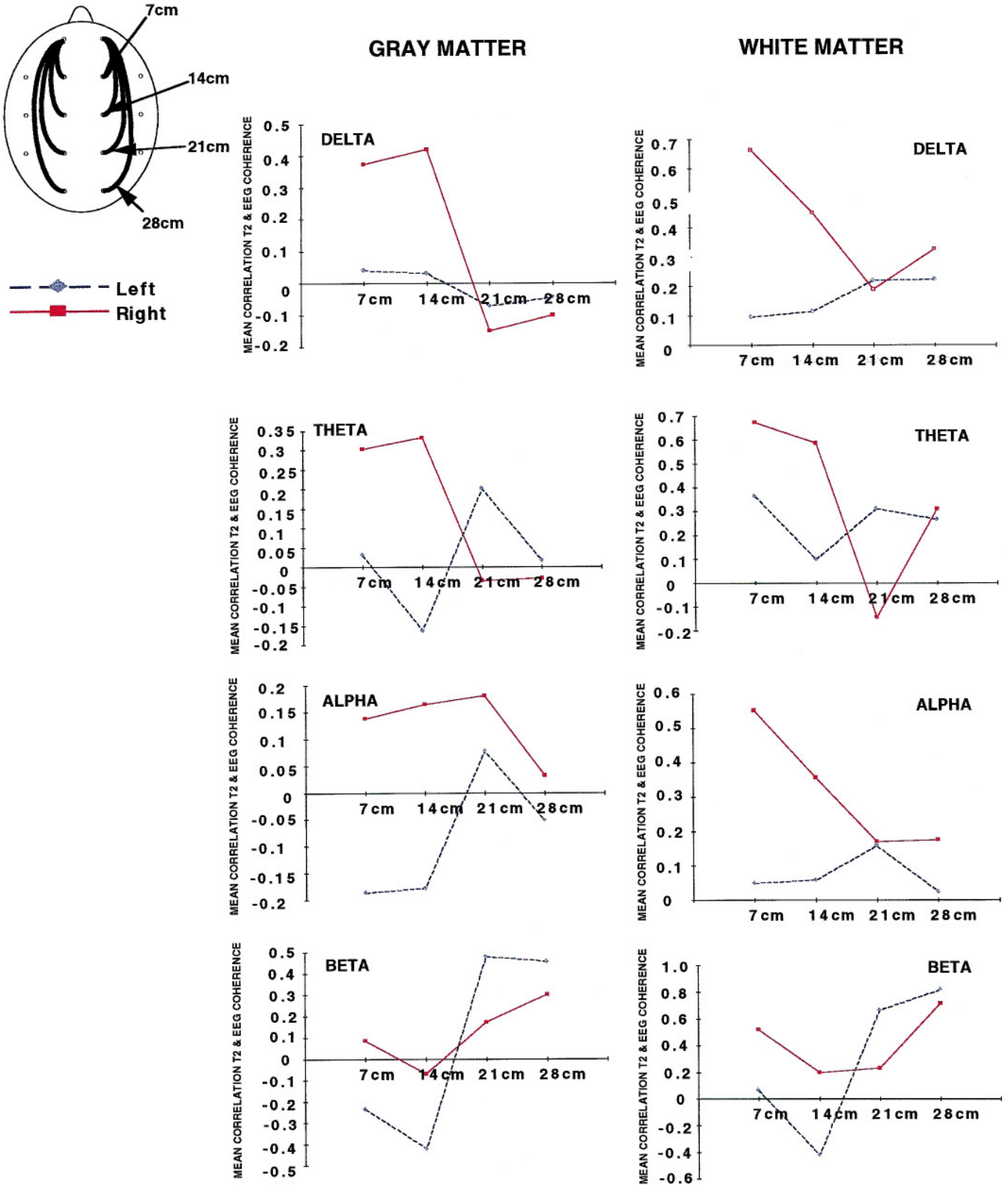

FIG. 7. Mean correlations between T2 relaxation times and EEG coherence in normal subjects. An illustration of the anterior-to-posterior electrode arrangement is shown at the top left. The left column are mean correlations between gray matter T2 relaxation time and EEG coherence and the right column are mean correlations between white matter T2 relaxation time and EEG coherence. The mean correlation is the average correlation between T2 relaxation time and EEG coherence for all 15 MRI slices (i.e., a 4.5-cm volume). Comparisons in mean correlation for the four different interelectrode distances (i.e., 7, 14, 21, and 28 cm) are shown on the x-axis. Unlike the CHI patients (Figs. 3, 4, and 5) polarity reversals in mean correlation were not present in the lower EEG frequencies (e.g., delta or theta). However, polarity reversals in mean correlation between T2 relaxation time and EEG coherence were present in the beta frequency band, especially from the left hemisphere.

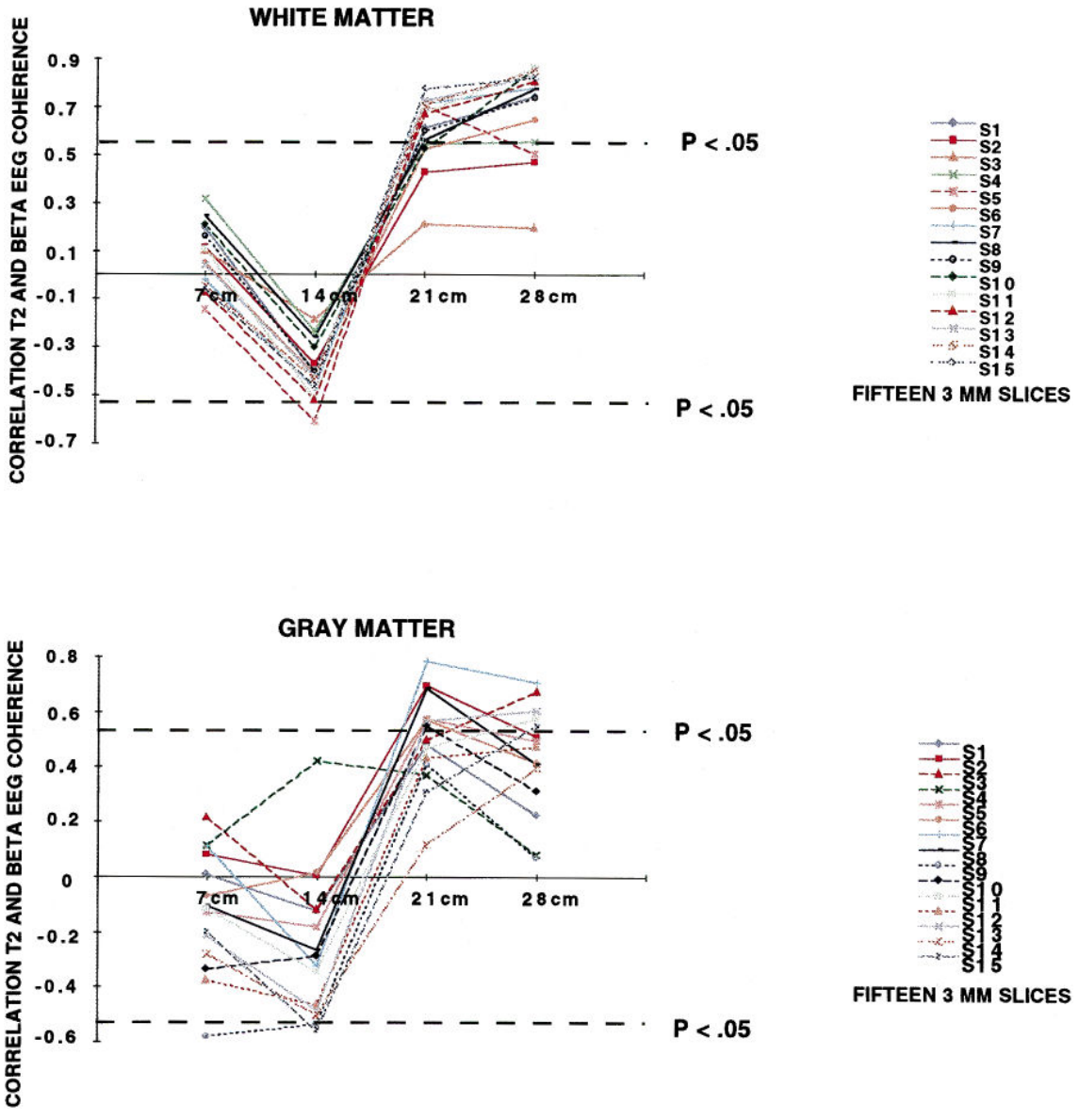

FIG. 8. Beta EEG coherence correlations with T2 relaxation time in normal subjects. The top graph shows the superimposed correlations between white matter T2 relaxation time and left hemisphere beta EEG coherence for all 15 slices from Fig. 7. The bottom graph shows the superimposed correlations between gray matter T2 relaxation time and left hemisphere beta EEG coherence for all 15 slices from Fig. 7. The x-axis is the interelectrode distances in centimeters and the y-axis is the individual correlation values. The dashed lines show the probability value of the correlation at $P < 0.05$. Polarity reversal in T2 relaxation time correlation with EEG coherence is evident between the short (e.g., 7 or 14 cm) interelectrode distances and the long (e.g., 21 or 28 cm) interelectrode distances in normal subjects.

and are myelinated and constitute as a distinguishing characteristic, the cortical white matter. Nunez and Katznelson (Nunez, 1981) were the first to suggest a possible relationship between EEG coherence and Braitenberg's cortical anatomical model. The precision of these concepts was experimentally tested and the first mathematical two-compartmental model of human EEG coherence shown in Fig. 9 was proposed in 1986 (Thatcher *et al.,* 1986). The mathematical model was $EEG\ Coherence = Ae^{-kx} + Be^{kx} \sin x$ (see Fig. 9), where A, B are constants, k is a function of frequency, and x is interelectrode distance in cm. Nonlinear regression analysis accounted for 99% of the variance of measured alpha coherence in a population of 189 subjects (Thatcher *et al.,* 1989). Pascual-Marqui *et al.* (1988) independently confirmed this equation and extended it to all EEG frequencies. In the past 10 years the existence of a short vs long distance "two-compartmental model" of EEG coherence has received considerable experimental and mathematical support (Nunez, 1994; Pascual-Marqui *et al.,* 1988; Wright, 1997; Petsche, 1996; Van Baal, 1997) and may also help explain the

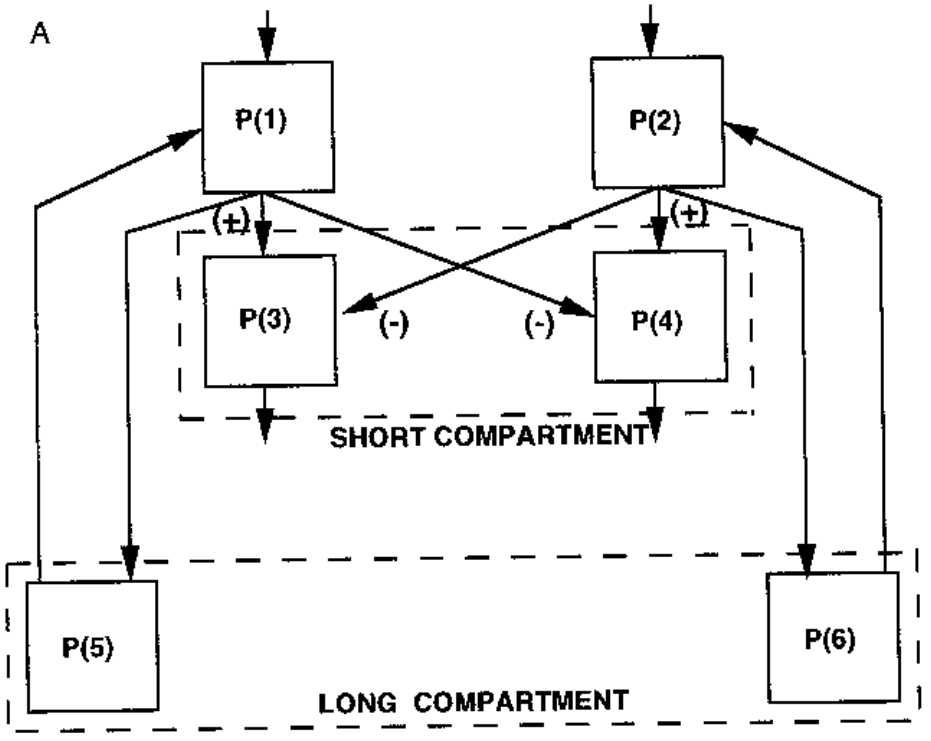

$$\text{Coherence} = Ae^{-kx} + Be^{kx}\sin x$$

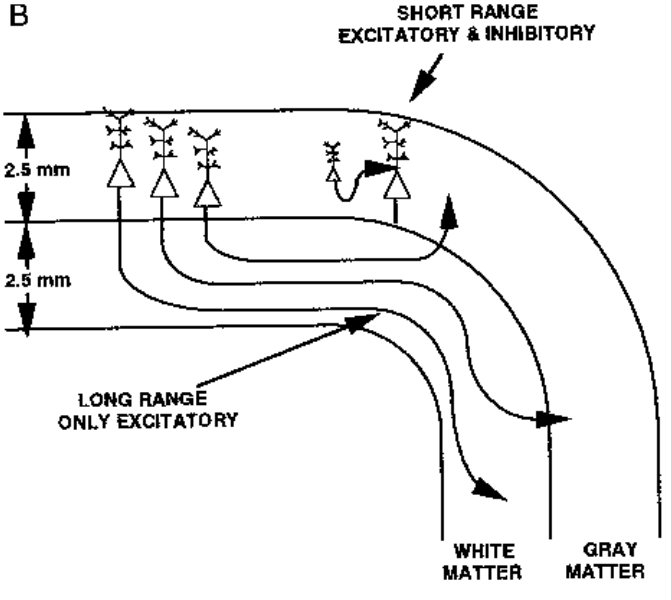

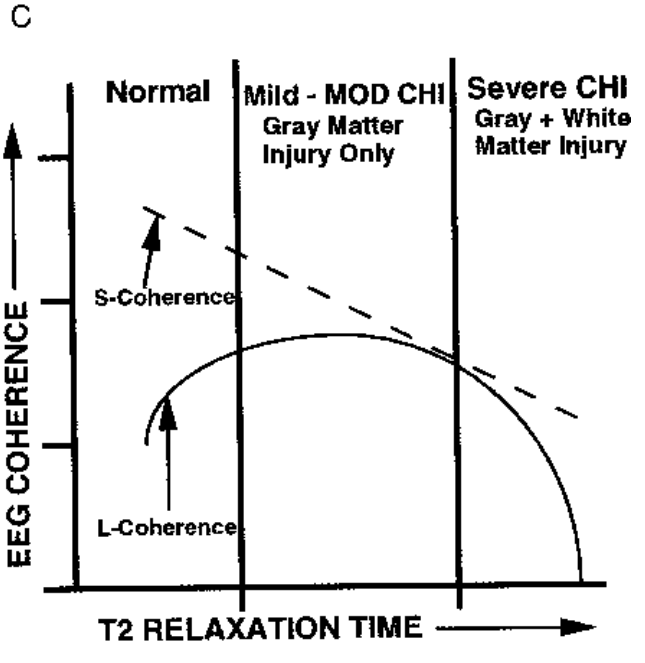

findings of this study. For example, according to the two-compartmental model of EEG coherence short- and long-distance EEG coherence reflect the operation of two distinctly different compartments, the short distance compartment (Ae^{-kx}) is dominated by cortico-cortical connections that reside within the gray matter and tend to exhibit a "diffusive" spatial dynamic described by the negative exponential while the long-distance compartment (Be^{kx} sin$x$) is dominated by myelinated long-distance cortico-cortical connections that tend to exhibit a "feedback" loop spatial dynamic (Nunez, 1981, 1994; Thatcher, 1992, 1994; Wright, 1997; Van Baal, 1997). The two compartments appear to be dynamically linked and often exhibit competitive relationships in which changes in EEG coherence in the two compartments are inversely related (Thatcher *et al.,* 1986; Thatcher, 1994, 1998). The competitive dynamics are mathematically modeled by assuming that neural populations can communicate with their local neighbors but that there is a trade off for simultaneous communication with long distance neighbors, including a dynamic oscillatory balance between the influences of the short- and long-distance systems (Thatcher, 1998). Recent identical twin studies have provided further support for the operation of short- and long-distance EEG coherence compartments by demonstrating possible independent heritabilities for the two compartments (van Baal, 1994). In the van Baal longitudinal study of 209 twin pairs, for example, EEG coherence from short-distance interelectrode (e.g., 6 to 7 cm) exhibited approximately 40% heritabilities, whereas EEG coherence from the long-distance interelectrodes (e.g., 28 cm) exhibited approximately 70% heritabilities (van Baal, 1994).

4.2 Biophysical Linkage between EEG Coherence and T2 Relaxation Time

It is well-established that $T2$ relaxation time is a biophysical measure of ^{1}H or water proton dynamics of the protein/lipid structures of the brain (Bottomley *et al.,* 1984; Wehrli, 1992). Therefore, a hypothesized biophysical linkage between $T2$ relaxation time and EEG coherence may be postulated by linking together the two-compartmental model of EEG coherence with $T2$ relaxation time. The goal of postulating a hypothesis is not to affirm a direct and causal linkage between ^{1}H and EEG coherence but, rather, hopefully to stimulate future investigations of the correlations between $T2$ relaxation and EEG coherence. An hypothesized biophysical linkage occurs if one assumes that: (1) that there are spatial gradients of injury in which frontal gray matter is the most injured with white matter less injured; (2) lengthened $T2$ is due to a reduction in the molecular integrity of the protein/lipid membranes of cortical neurons thus reducing electrophysiological efficiency and effectiveness, and (3) reduced short-distance EEG coherence reflects reduced efficiency and effectiveness of cortico-cortical communication. A simple mathematical linkage is found in the nonlinear dynamics of ecological systems involving predator/prey, competition, and cooperation (Berryman, 1981). According to the competitive and predator-prey mathematical model of EEG coherence, reduced EEG coherence in the local domain results in increased coherence in the long-distance domain (Thatcher *et al.,* 1986; Thatcher, 1998). For example, it would be consistent with a nonlinear dynamic model of EEG coherence for biomechanically induced gray matter injury to result in reduced effectiveness of communication within the "alpha" or short-distance connection system as reflected by reduced EEG coherence in short interelectrode distances. As a consequence of the competitive relationship between the short- and long-distance systems reduced short-distance coupling in mild to moderate brain injury necessarily results in increased long-distance coupling because the long-distance connection systems are relatively intact or less injured than the short-distance connections, thus winning in the competitive interac-

FIG. 9. Hypothesized linkage between T2 relaxation time and EEG coherence. (A) The mathematical "two compartmental" model of EEG coherence by Thatcher *et al.* (1986) and Pascual-Marqui *et al.* (1988) in which nonlinear regression analyses demonstrated 90 to 99% accuracy of fit to human EEG coherence measurements. P(1) and P(2) are two different populations of cells located within the cortical gray matter that are synaptically connected by excitatory (+) and inhibitory (−) inputs to their "local" neighboring cells (P(3) and P(4) which are also located within the gray matter. This serial competitive feedback circuit represents the local connection compartment or alpha system "A" which exhibits a "diffusive" spatial dynamic. The long-distance fiber compartment is represented by the cells in populations P(1) and P(2) that map to cells in populations P(5) and P(6) in which there is a "feedback" or return loop from population P(5) and P(6) to P(1) and P(2), respectively. This reciprocal feedback system represents the long distance connection compartment of beta system "B." (B) A diagrammatic illustration of the neocortical white matter and gray matter where long-distance and myelinated axons travel and which exclusively exhibit excitatory input to the various layers of the neocortex. In contrast, the short-distance connections of the gray matter are both excitatory and inhibitory (e.g., inhibition from interneurons) and the inhibitory interneurons do not send axons into the white matter. (C) The hypothesized relationship between T2 relaxation time and EEG coherence. In C normal subjects exhibit a range of short- and long-distance EEG coherence dynamics as a function of T2 relaxation time (especially in the beta frequency band, see Fig. 8), following mild and moderate traumatic brain injury then short-distance EEG coherence declines and long-distance EEG coherence increases (especially in the lower EEG frequencies, see Figs. 2, 3, 4, and 5), and with severe traumatic brain injury there is a continued decline in short-distance EEG coherence with an eventual sharp decline in long-distance EEG coherence as the myelinated axons of the white matter are severely damaged.

tion. For purposes of clarity, Fig. 9 illustrates this hypothesis in which Fig. 9A is the "two-compartmental" model of EEG coherence (Thatcher *et al.,* 1986; Pascual-Marqui *et al.,* 1988) and Fig. 9B illustrates the cortical architecture of the short- and long-distance compartments, while Fig. 9C illustrates the hypothesized relationship between $T2$ relaxation time and EEG coherence. In Fig. 9C normal subjects exhibit a range of short- and long-distance EEG coherence dynamics as a function of $T2$ relaxation time (especially in the beta frequency band), following mild and moderate traumatic brain injury short-distance EEG coherence markedly declines and long-distance EEG coherence increases (especially in the lower EEG frequencies) and with severe traumatic brain injury there is a continued decline in short-distance EEG coherence with an eventual sharp decline in long-distance EEG coherence as the myelinated axons of the white matter are severely damaged. It is experimentally feasible to test such a model in animal preparations.

A second hypothesis is that decreased short-distance EEG coherence and increased long-distance EEG coherence are a functional compensatory process in which the response to injury of the gray matter is increased functional differentiation, indicated by decreased short-distance EEG coherence and increased long-distance integration indicated by increased long-distance EEG coherence. While such a compensatory process is possible, nonetheless, it fails to explain the presence of competitive relationships between short- and long-distance EEG coherence observed in normal and intact individuals (Nunez, 1981; 1994; Thatcher *et al.,* 1986; Thatcher, 1994, 1995; Fig. 8). Importantly, one would expect that neuropsychological tests of cognitive function could help clarify this issue by either supporting or rejecting these alternatives. The compensatory hypothesis states that decreased short-distance EEG coherence is an adaptive reorganization, which helps compensate for brain damage and, therefore, neuropsychological test scores should be *negatively* related to short-distance EEG coherence, i.e., as short-distance EEG coherence declines then cognitive performance improves. On the other hand, according to the membrane integrity hypothesis, decreased short-distance EEG coherence is due to injury to the protein/lipid molecules of the brain, therefore, neuropsychological test scores should be *positively* related to short-distance EEG coherence, i.e., as short-distance EEG coherence increases then cognitive performance improves. The results of the present study support the membrane integrity hypothesis by multivariate analyses of variance (Table 3) as well as linear regression analyses (Fig. 6), which revealed consistent *positive* relationships between declining cognitive performance and decreased short-distance EEG coherence.

4.3 Frequency Dependence and T2 Relaxation Time

A marked EEG frequency disparity was present in the comparison between both groups of CHI patients and the normal controls. CHI patients exhibited polarity reversals in correlation in the delta and theta frequency bands as a function of distance, with no or weak polarity reversals in the beta frequency band. In contrast, the normal control subjects failed to exhibit lower frequency polarity reversals but did exhibit clear and strong polarity reversals in the beta frequency band (Figs. 7 and 8). It is difficult to argue that this observed frequency shift is due simply to sampling error or a reduced "effect size" or poor signal-to-noise ratio, etc. Instead, the findings demonstrate the same short- versus long-distance EEG coherence inverse relation in normal subjects but at a higher frequency than in the CHI patients. This finding can be explained by a single hypothesis that assumes: (1) a short- versus long-distance competitive dynamic in which the most efficient communication channels are in the higher frequency domain as exhibited by the normal control subjects and (2) that the competitive "two-compartmental" process is still operative in CHI patients but only at lower frequencies. In other words, brain injury results in reduced efficiency and reduced dynamical speed, i.e., "a slowing" of the two-compartmental competition. This hypothesis is also consistent with the observed correlation between $T2$ relaxation time and EEG amplitude and frequency (Thatcher *et al.,* 1998). The biophysical details of the correlation between EEG coherence and $T2$ relaxation time will require additional investigation, especially of the relationship between scalp recorded EEG and ^{1}H and ^{31}P spectroscopy and tensor diffusion-weighted imaging in smaller volumes of the brain.

ACKNOWLEDGMENTS

We acknowledge the data analysis and editorial assistance of Rebecca Walker, Richard Curtin, and Duane North. We are also indebted to Drs. Glen Curtis, Rodney Vanderploog, and Rex Bierley for discussions of the neuropsychological tests and Ms. Kathleen Haedt for administering the neuropsychological tests. We are also indebted to Dr. J. C. Daniel's efforts in arranging for the acquisition of MR images in the normal control subjects. This project was supported by Contract No. JFC36285006 as part of the Department of Defense and Veterans Head Injury Program (DVHIP). Informed consent was obtained from all subjects in this study.

APPENDIX A

The calculation of $T2$ relaxation time is based on the fact that $TR_{T2} = TR_{PD}$, thus:

$$\frac{I_{T2}}{I_{PD}} = \frac{KN(1 - e^{-TR_{T2}/T1})e^{-TE_{T2}/T2}}{KN(1 - e^{-TR_{T2}/T1})e^{-TE_{PD}/T2}}, \qquad \text{Eq 1}$$

since K, N, TR_{T2}, TR_{PD} cancel, then Eq. 1 can be simplified to EQ 2,

$$\frac{I_{T2}}{I_{PD}} = e^{\frac{(TE_{PD} - TE_{T2})}{(T2)}} \qquad \text{Eq 2}$$

By taking the log of the ratio we obtain:

$$\ln\left(\frac{I_{T2}}{I_{PD}}\right) = \frac{TE_{PD} - TE_{T2}}{T2}, \qquad \text{Eq 3}$$

and then by rearranging to solve for $T2$:

$$T2 = \frac{TE_{PD} - TE_{T2}}{\ln\,(I_{T2}/I_{PD})}, \qquad \text{Eq 4}$$

where I_{T2} and I_{PD} are the pixel intensities from the respective $T2$ and PD images.

REFERENCES

Bendat, J. S., and Piersol, A. G. 1980. *Engineering Applications of Correlation and Spectral Analysis.* Wiley, New York.

Bensaid, A. M., Hall, L. O., Bezdek, J. C., and Clarke, L. P. 1994. Fuzzy cluster validity in magnetic resonance images. In *Medical Imaging: Image Processing. Proceedings SPIE* (M. H. Loew, Ed.), 2167, pp. 454–464.

Berryman, A. A. 1981. *Population Systems: A General Introduction.* Plenum Press, New York.

Bezdek, J. C., Hall, L. O., and Clarke, L. P. 1993. Review of MR image segmentation techniques using pattern recognition. *Med. Phys.* **20:**1033–1048.

Bloch, F. 1946. Nuclear induction. *Phys. Rev.* **70:**460–482.

Bottomley, P. A., Foster, T. H., Argersinger, R. E., and Pfeifer, L. M. 1984. A review of normal tissue hydrogen NMR relaxation times and relaxation mechanisms from 1-100 Mhz: Dependence on tissue type, NMR frequency, temperature, species, excision and age. *Med. Phys.* **11**(4):425–448.

Bottomley, P. A., Hardy, C. J., Argersinger, R. E., and Allen-Moore, G. 1987. A review of ^{1}H nuclear magnetic resonance relaxation in pathology: Are T_1 and T_2 diagnostic? *Med. Phys.* **14:**1–36.

Braitenberg, V. 1978. Cortical architectonics: General and areal. In *Architectectonics of the Cerebral Cortex* (M. A. B. Brazier and H. Petsche, Eds.) Academic Press, New York.

Braitenberg, V., and Schuz, A. 1991. *Anatomy of the Cortex: Statistics and Geometry.* Springer, Berline Heidelberg New York.

Clarke, L. P., Velthuizen, R. P., Camacho, M. A., Heine, J. J., Vaidyanathan, M., Hall, L. O., Thatcher, R. W. and Silbiger, M. L. 1995. MRI Segmentation: Methods and applications. *Mag. Res. Imag.* **13:**343–368.

Cohen, J., and Cohen, P. 1983. *Applied Multiple Regression/Correlation Analysis for the Behavioral Sciences.* Erlbaum, New Jersey.

Daniel, J. C., Reeves, D., Tam, D. A., Bleiberg, J., and Thatcher, R. W. 1997. Correlates of sports concussion in adolescents. In *Defense and Veterans Head Injury Program Project.* Henry Jackson Foundation, Washington, D. C.

Darwin, R. H., Drayer, B. P., Riederer, S. J., Wang, H. Z., and MacFall, J. R. 1986. T2 estimates in healthy and diseased brain tissue: A comparison using various MR pulse sequences. *Radiology* **160:**375–381.

De Certaines, J. D., Henriksen, O., Spisni, A., Cortsen, M., and Ring, P. B. IV. 1993. *In vivo* measurements of proton relaxation times in human brain, liver, and skeletal muscle: A multicenter MRI study. *Mag. Reson. Imag.* **11:**841–850.

Dixon, R. L., and Ekstrand, K. E. 1982. The physics of proton NMR. *Med. Phys.* **9:**807–818.

Fein, G., Raz, J., Brown, F. F., and Merrin, E. L. 1988. Common reference coherence data are confounded by power and phase effects. *EEG Clin. Neurophysiol.* **69:**581–584.

Fullerton, G. D. 1992. Physiological basis of magnetic relaxation. In *Magnetic Resonance Imaging* (D. D. Stark and W. G. Bradley, Eds.), Mosby Year Book, St. Louis, pp. 88–108.

Henriksen, O., De Certaines, J. D., Spisni, A., Cortsen, M., Muller, R. N., and Ring, P. B. V. 1993. *In vivo* measurements of proton relaxation times in human brain, liver, and skeletal muscle: A multicenter MRI study. *Mag. Reson. Imag.* **11:**811–856.

Hickley, D. S., Checkleyt, D., Aspden, R. M., Naughton, A., Jenkins, J. P., and Isherwood, I. 1986. A method for the clinical measurement of relaxation times in magnetic resonance imaging. *Br. J. Radiol.* **59:**565–576.

Koenig, S. H. 1991. Cholesterol of myelin is the determinant of gray-white contrast in MRI of brain. *Magn. Reson. Med.* **20:**285–191.

Kjos, O., Ehman, R. L., Brant-Zawadzki, M., Kelly, W. M., Normasn, D., and Newton, T. H. 1985. Reproducibility of relaxation times and spin density calculated from routine MR imaging sequences: Clinical study of the CNS. *Am. J. Radiol.* **144:**1165–1170.

Mills, C. M., Crooks, L. E., Kaufman, L., and Brant-Zawadzki, M. 1984. Cerebral abnormalities: Use of calculated T1 and T2 magnetic resonance images for diagnosis. *Radiology* **150:**87–94.

Nicholson, C. 1980. Dynamics of the brain cell microenvironment. *Neurosci. Res. Prog. Bull.* **18**(2):181–243.

Nicholson, C., and Phillips, J. M. 1981. Ion diffusion modified by tortuosity and volume fraction in the extracellular microenvironment of the rat cerebellum. *J. Physiol.* **321:**225–257.

Nunez, P. 1981. *Electrical Fields of the Brain.* Oxford Univ. Press, Cambridge.

Nunez, P. 1995. *Neocortical dynamics and human EEG rhythms.* Oxford Univ. Press, New York.

Nunez, P. L., Srinivasan, R., Westdorp, A. F., Wijesinghe, R. S., Tucker, D. M., Silberstein, R. B., and Cadusch, P. J. 1997. EEG coherency I: Statistics, reference electrode, volume conduction, Laplacians, cortical imaging and interpretation at multiple scales. *EEG Clin. Neurophysiol.* **103:**499–515.

Otnes, R. K., and Enochson, L. 1972. *Digital Time Series Analysis.* Wiley, New York.

Pascual-Marqui, R. D., S. L., Valdes-Sosa, P. A., and Alvarez-Amador, A. 1988. A parametric model for multichannel EEG spectra. *Int. J. Neurosci.* **40:**89–99.

Petsche, H. 1996. Approaches to verbal, visual and musical creativity by EEG coherence analysis. *Int. J. Psychophysiol.* **24:**145–159.

Rappelsberger, P. 1989. The reference problem and mapping of coherence: A simulation study. *Brain Topog.* **2**(1/2):63–72.

Savitzky, A., and Golay, M. J. E. 1964. Smoothing and differentiation of data by simplified least squares procedures. *Analytical Chemistry* **36:**1627–1639.

Schoeniger, J. S., Aiken, N., Hsu, E., and Blackband, S. J. 1994. Relaxation-time and diffusion NMR microscopy of single neurons. *J. Mag. Reson. Series B* **103:**261–273.

Szafer, A., Zhong, J., and Gore, J. C. 1995. Theoretical model for water diffusion in tissues. *Mag. Reson. Med.* **33:**687–712.

Thatcher, R. W., Krause, P., and Hrybyk, M. 1986. Corticocortical associations and EEG coherence: A two compartmental model. *Electroencephalogr. Clin. Neurophysiol.* **64:**123–143.

Thatcher, R. W., Walker, R. A., and Guidice, S. 1987. Human cerebral hemispheres develop at different rates and ages. *Science* **236:**1110–1113.

Thatcher, R. W., Walker, R. A., Gerson, I., and Geisler, F. 1989. EEG discriminant analyses of mild head trauma. *EEG Clin. Neurophysiol.* **73:**93–106.

Thatcher, R. W. 1992. Cyclic cortical reorganization during early childhood development. *Brain Cog.* **20:**24–50.

Thatcher, R. W. 1994. Psychopathology of Early Frontal Lobe Damage: Dependence on Cycles of Postnatal Development. *Dev. Pathol.* **6:**565–596.

Thatcher, R. W. 1995. Tomographic Electroencephalography and Magnetoencephalography. *J. Neuroimag.* **5:**35–45.

Thatcher, R. W., Camacho, M., Salazar, A., Linden, C., Biver, C., and Clarke, L. 1997. Quantitative MRI of the gray-white matter distribution in traumatic brain injury. *J. Neurotrauma* **14:**1–14.

Thatcher, R. W., Biver, C., Camacho, M., McAlaster, R., and Salazar, A. M. 1998. Biophysical linkage between MRI and EEG amplitude in closed head injury. *NeuroImage* **7**(4):352–367.

Thatcher, R. W. 1998. A predator/prey model of human cerebral development. In *Dynamical Systems and Development* (K. Newel and P. Molennar, Eds.) Lawrence Erlbaum, Hillsdale, NJ.

van Baal, C. 1997. *A Genetic Perspective on the Developing Brain.* Dissertation, VRIJE University, The Netherlands Organization for Scientific Research (NWO). [ISBN: 90-9010363-5].

Velleman, P. F. 1995. Data Desk: Version 5.0. Data Description, Inc. Ithaca, New York.

Wehrli, F. W. 1992. Principles of magnetic resonance. In *Magnetic Resonance Imaging* (D. D. Stark and W. G. Bradley, Eds.), pp. 3–20. Mosby Year Book, St. Louis.

Wright, J. J. 1997. EEG simulation: variation of spectral envelope, pulse synchrony and 40 Hz oscillation. *Biol. Cybernet.* **76:**181–194.